Electronic supplementary information (ESI)

Systematic Study of Interdependent Relationship on Gold Nanorod Synthesis Assisted by Electron Microscopy Image Analysis

Seokyoung Yoon,[a] Byoungsang Lee,[b] Jaesub Yun,[c] Jeon Geon Han,[b] Jong-Seok Lee,[*c] Jung Heon Lee[*a,b]

[a]SKKU Advanced Institute of Nanotechnology (SAINT), [b]School of Advanced Materials Science and Engineering, and [c]Department of Systems Management Engineering, Sungkyunkwan University (SKKU), Suwon 16419, South Korea

Corresponding Authors:

*JSL: E-mail: jongseok@skku.edu, Tel: +82-31-290-7608, Fax: +82-31-290-7610

*JHL: E-mail: jhlee7@skku.edu, Tel: +82-31-290-7404, Fax: +82-502-302-1918

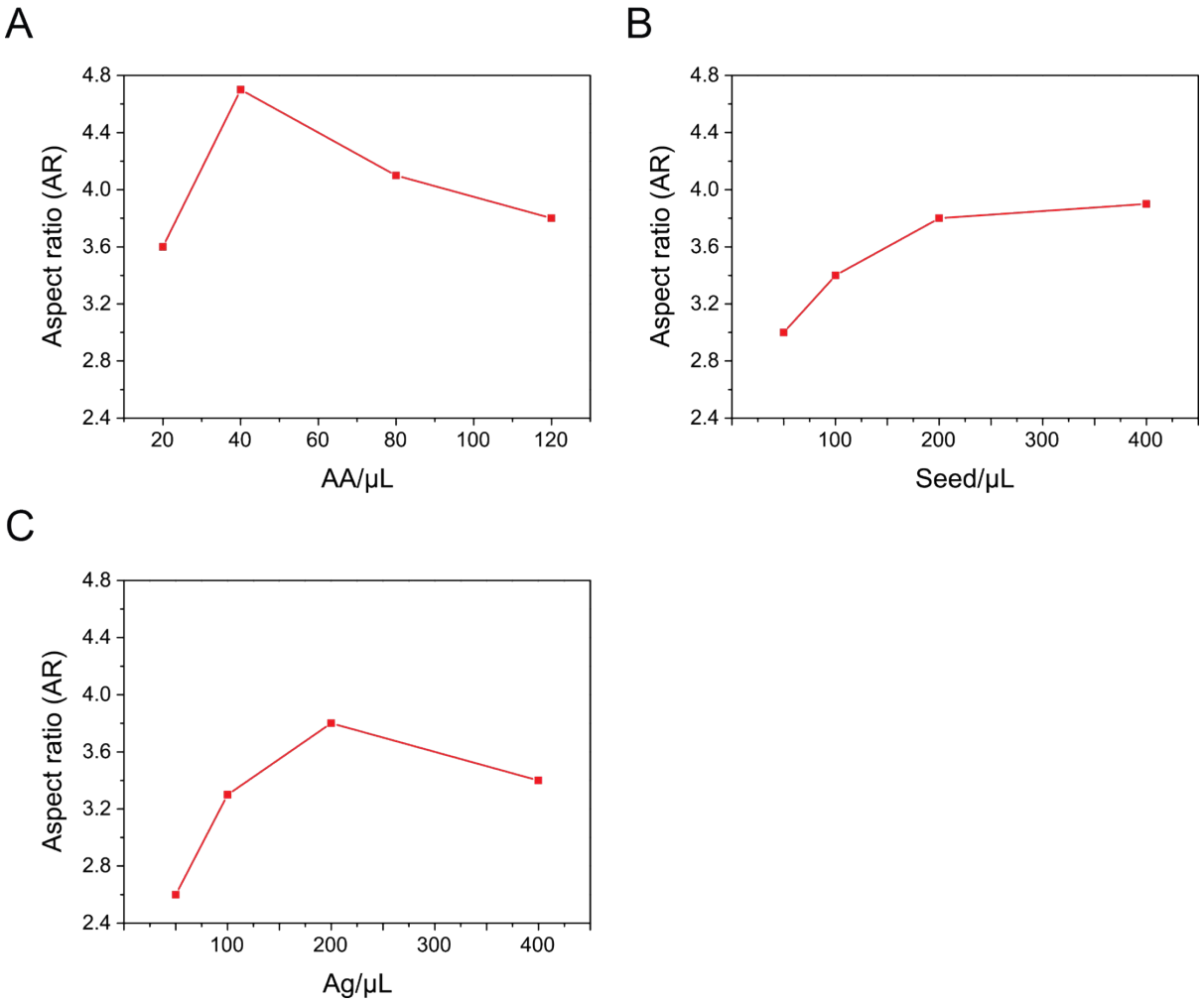

Figure S1. Aspect ratio (AR) variation of GNRs synthesized with various amounts of (A) AA, (B) seed, and (C) silver ion. Since LSPR peak position of a GNR is related to its AR, the trend of each AR curve correlates well with the trend of LSPR peak position from Fig. 1C, Fig. 2B, Fig. 3B.

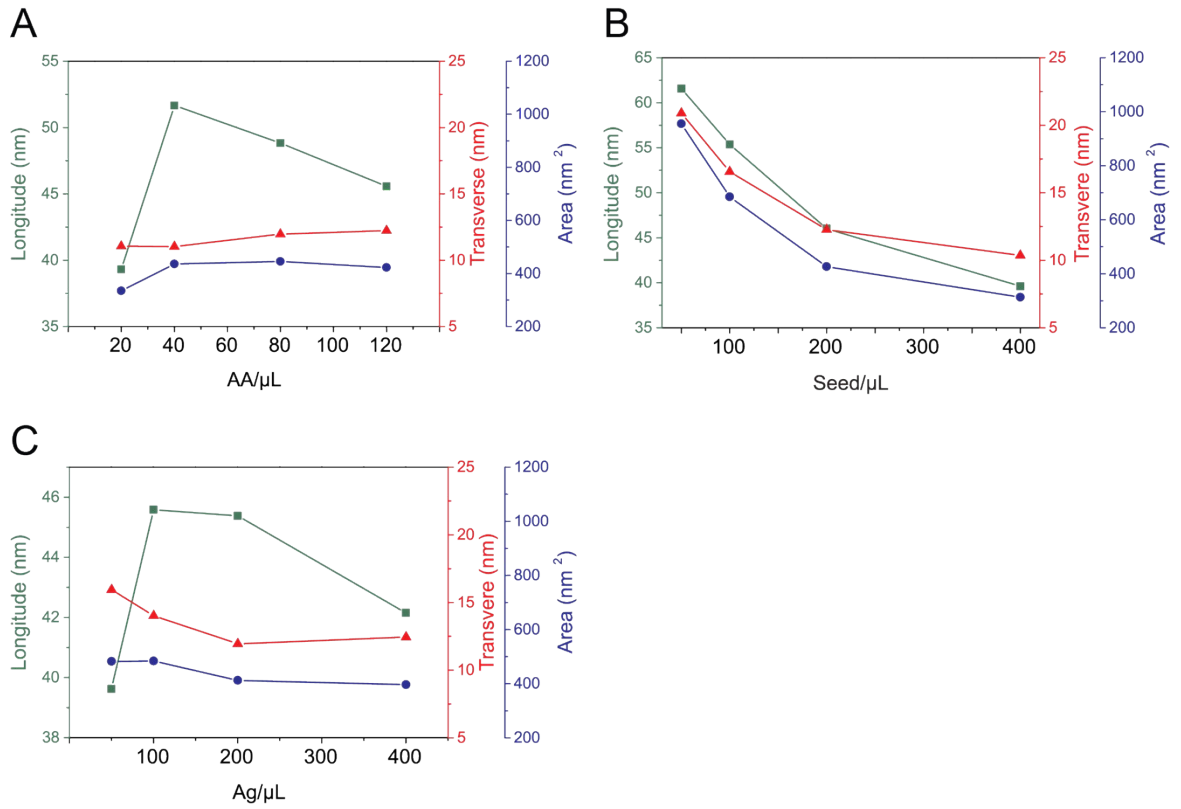

Figure S2. The dimension of all the GNRs synthesized under different synthetic conditions were analyzed using TEM image analysis. (A) The longitudinal length significantly changed as the amount of AA varied, while the transverse length did not. (B) Both longitudinal and transverse lengths as well as the area of GNRs were inversely proportional to the amount of seed. (C) Both longitudinal and transverse lengths of GNR changed simultaneously. The area of GNR slightly decreased as the amount of Ag ion increased.

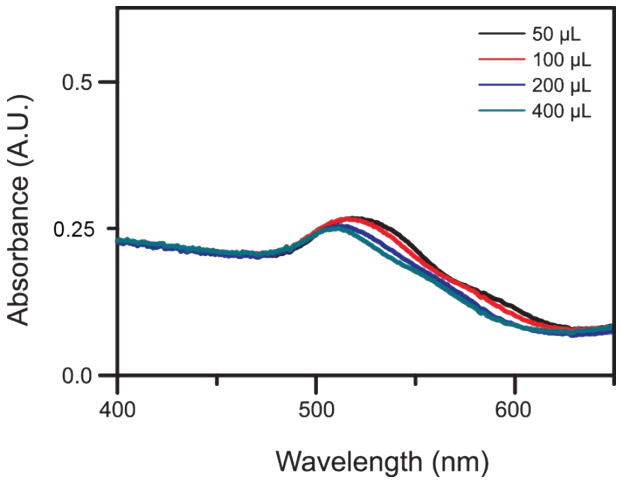

Figure S3. A magnified figure of the changes in spectra at around 400-650 nm in Fig.2C in the manuscript. Transverse localized surface plasmonic resonance peak appeared broadened with the low amount seed, as shown with $GNR_{50\ \mu L\ seed}$ and $GNR_{100\ \mu L\ seed}$.

TEM image analysis and solidity

The images were obtained from TEM and analyzed by a custom MATLAB script with some subroutine implemented in the image processing toolbox of MATLAB. There was a big hurdle to analyze all TEM images using a single thresholding technique, required to separate nanoparticles from background. This is because the images of the nanoparticles and the background are not uniform in every TEM image (Fig. S4A). As a result, after thresholding and pretreatment, we would get the results containing misidentified noises, such as very small or indeterminate form of nanoparticles, even though original TEM image does not contains such objects (Red circles in Fig. S4C). This noises can lead to false image analysis of nanoparticles. Therefore, we separated the nanoparticles from the background using various thresholding and pretreatment techniques.

First, a preprocessing algorithm was run on a TEM image. It was used to reduce the effect of background by using a low-pass filter, a histogram equalization, and an imclearborder subroutine (Fig. S4B). Next, a Canny edge detector, a Laplacian of Gaussian edge detector, and a zerocross subroutine were run with imfill subroutine that filled closed regions. As a result, we were able to obtain candidate images with significantly less noising objects. (Fig S4C). Next, to get even better result, noises with a solidity value of under 80% and area smaller than 100 pixels were cleared from candidate images (Fig S4D). Finally, a regionprops subroutine was run to quantify the area and the solidity of each particle.

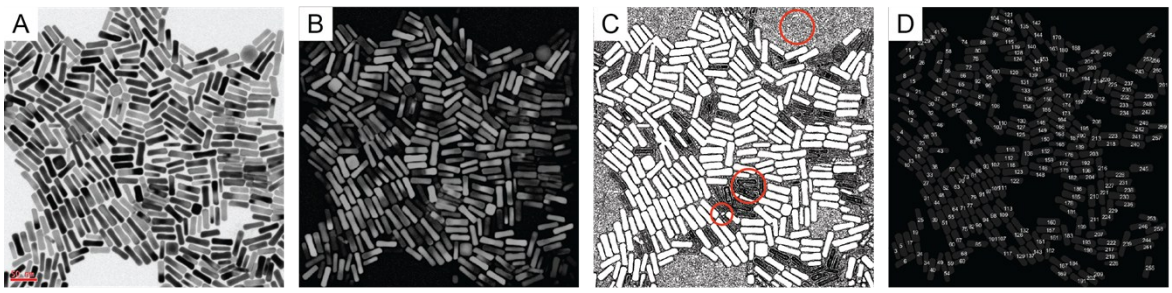

Figure S4. TEM image analysis process: (A) An image of nanoparticles taken with TEM. (B) The image ran with preprocessing algorithm. (C) Image of filled edge containing nanoparticles and noise. Red circles contain noise objects. (D) The final image after noise removal.

Table S1. Summary of the reaction conditions and the characteristics of GNRs investigated with various amounts of AA, seed, and silver ion.

$AgNO_3$ solution (μL)	Ascorbic acid solution (μL)	Seed (uL)	Average dimensions measured by TEM (nm)	Solidity	AR_{avg}	λ_{LSPR} (nm)	Intensity at λ_{LSPR}	As-synthesized concentration	Total counts	Impurity counts	Impurity (%)
200	20	200	39.3 ± 6.4 11.0 ± 1.3	0.964	3.6	804	0.36	0.144 nM	1574	25	1.59
200	40	200	51.7 ± 7.8 11.0 ± 1.4	0.958	4.7	882	0.83	0.282 nM	1013	26	2.57
200	80	200	48.8 ± 6.2 12.0 ± 1.8	0.945	4.1	835	1.12	0.443 nM	1635	51	3.12
200	120	200	45.6 ± 6.1 12.2 ± 1.7	0.940	3.8	812	1.23	0.494 nM	1653	33	1.99
200	120	50	61.6 ± 8.6 20.9 ± 3.8	0.910	3.0	775	1.11	0.480 nM	537	33	6.12
200	120	100	55.4 ± 6.3 16.6 ± 2.3	0.921	3.4	797	1.17	0.486 nM	1259	51	4.05
200	120	200	46.0 ± 5.6 12.3 ±1.5	0.939	3.8	812	1.20	0.481 nM	1591	66	4.15
200	120	400	39.6 ± 4.7 10.3 ± 1.2	0.957	3.9	812	1.21	0.486 nM	2105	57	2.71
50	120	200	39.6 ± 7.3 15.9 ± 2.4	0.976	2.6	712	0.62	0.327 nM	1596	55	3.45
100	120	200	45.6 ± 6.3 14.0 ± 2.1	0.950	3.3	775	0.96	0.422 nM	1430	67	4.69
200	120	200	45.4 ± 6.5 12.0 ± 1.8	0.937	3.8	810	1.24	0.501 nM	1877	43	2.29
400	120	200	42.2 ± 5.2 12.4 ± 1.5	0.946	3.4	774	1.05	0.462 nM	1441	99	6.87

The percentages of impurities are usually lower than ~5%, except for the reaction conditions with extremely large amount of seed or silver ion.

The intensity of the GNRs at LSPR peak position was measured with 1/2 times diluted GNRs.

Table S2. Summary of the reaction conditions investigated for optimal GNR synthesis.

$AgNO_3$ solution (μL)	Ascorbic acid solution (μL)	Seed (uL)	Average dimensions measured by TEM (nm)	Total counts	Impurity counts	Impurity (%)
120	80	50	66.2 ± 8.7 25.1 ± 4.5	516	30	5.81
120	90	50	64.8 ± 12.8 24.5 ± 8.5	469	43	9.17
120	100	50	71.3 ± 12.7 29.1 ± 7.7	760	80	10.53
120	110	50	68.9 ± 15.0 27.0 ± 7.9	527	45	8.54
120	120	50	64.7 ± 9.7 23.8 ± 4.7	551	37	6.72
120	130	50	69.3 ± 14.4 28.9 ± 7.5	964	105	10.90
120	140	50	65.3 ± 14.0 25.3 ± 7.9	894	57	6.38
120	150	50	67.6 ± 13.5 25.9 ± 7.6	1190	133	11.18
120	160	50	66.9 ± 14.5 27.1 ± 7.5	391	50	12.79
120	80	100	66.4 ± 8.7 25.8 ± 4.6	748	45	6.02
120	90	100	57.2 ± 9.0 18.2 ± 4.0	749	27	3.60
120	100	100	62.4 ± 10.2 22.6 ± 5.4	594	37	6.23
120	110	100	62.0 ± 10.5 21.6 ± 5.8	643	30	4.67
120	120	100	55.8 ± 8.2 18.8 ± 4.2	769	36	4.68
120	130	100	58.0 ± 12.4 21.8 ± 6.8	1066	79	7.41
120	140	100	60.0 ± 11.9 22.3 ± 7.0	508	21	4.13
120	150	100	54.1 ± 12.2 20.1 ± 5.3	534	39	7.30
120	160	100	56.4 ± 9.5 20.6 ± 5.9	505	26	5.15
120	80	200	54.8 ± 9.3 16.7 ± 3.4	780	24	3.08
120	90	200	52.5 ± 9.2 17.2 ± 4.2	878	64	7.29
120	100	200	54.6 ± 10.3 18.6 ± 4.9	516	32	6.20
120	110	200	56.7 ± 9.2 19.2 ± 4.3	571	24	4.20
120	120	200	53.0 ± 9.4 17.2 ± 4.4	570	20	3.51
120	130	200	53.1 ± 9.8 18.0 ± 4.5	610	23	3.77
120	140	200	53.8 ± 9.6 19.2 ± 5.2	547	28	5.12
120	150	200	56.2 ± 9.3 20.2 ± 4.6	507	30	5.92
120	160	200	50.3 ± 9.9 17.2 ± 5.2	655	29	5.53
120	80	400	48.3 ± 8.4 14.1 ± 2.9	1394	62	4.45
120	90	400	49.6 ± 9.4 15.1 ± 3.5	641	31	4.84
120	100	400	48.11 ± 9.7 14.9 ± 3.3	629	27	4.29
120	110	400	50.9 ± 8.2 16.2 ± 3.5	705	31	4.40
120	120	400	45.9 ± 9.2 14.7 ± 3.8	738	35	4.74
120	130	400	48.2 ± 8.2 16.2 ± 3.4	720	36	5.00

120	140	400	47.7 ± 8.0 15.5 ± 3.4	571	21	3.68
120	150	400	45.9 ± 8.5 14.8 ± 3.9	772	31	4.02
120	160	400	46.1 ± 7.9 15.2 ± 3.5	705	30	4.26

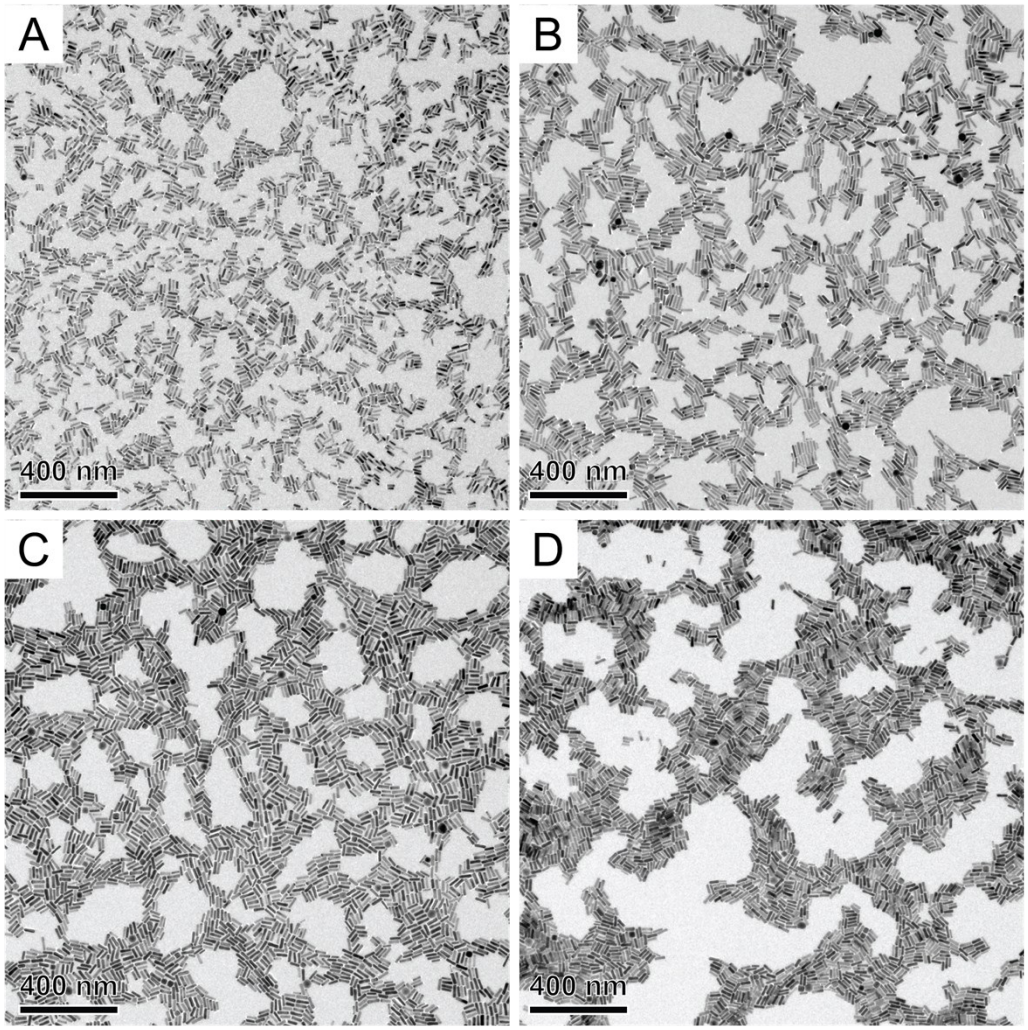

Figure S5. Low magnification TEM images of GNRs synthesized with various amounts of AA. (A) $GNR_{20\ \mu L\ AA,}$ (B) $GNR_{40\ \mu L\ AA,}$ (C) $GNR_{80\ \mu L\ AA,}$ and (D) $GNR_{120\ \mu L\ AA}$.

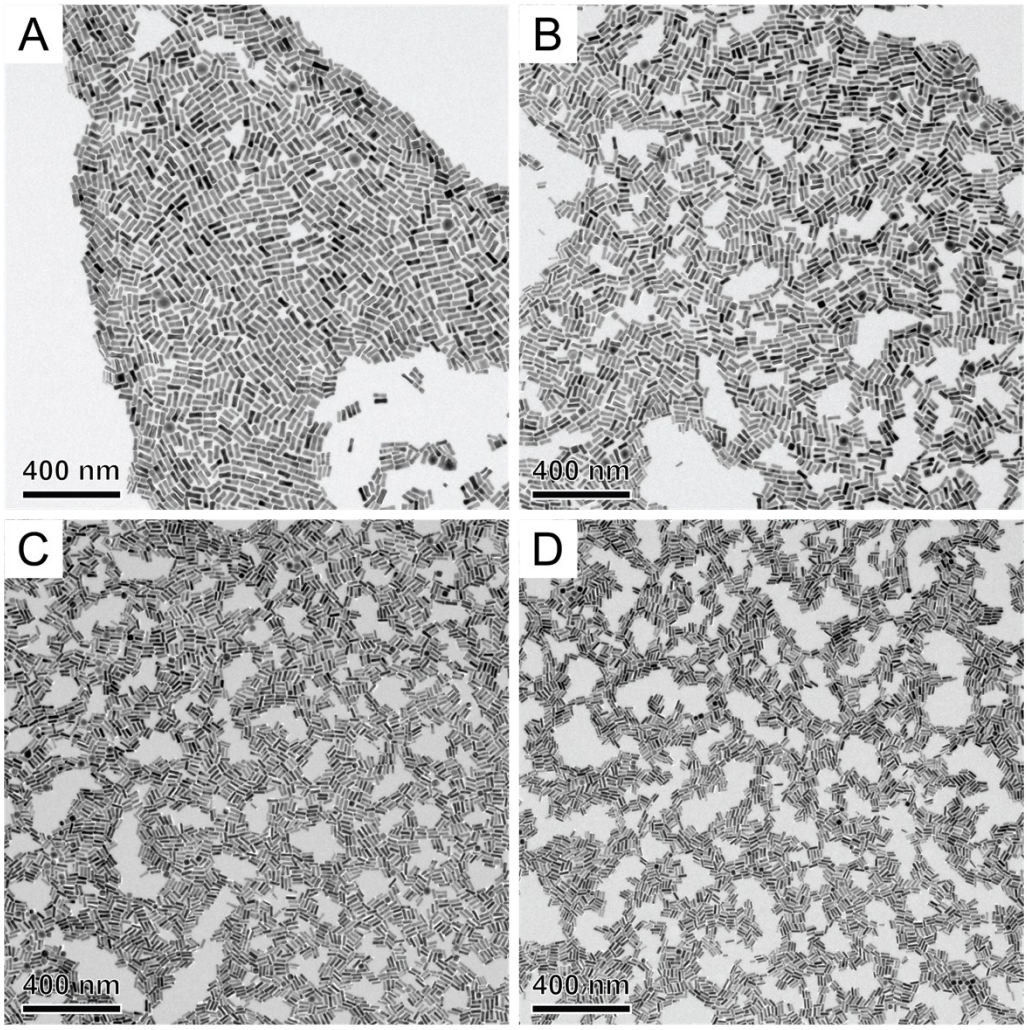

Figure S6. Low magnification TEM images of GNRs synthesized with various amounts of seeds. (A) $GNR_{50\ \mu L\ seed}$, (B) $GNR_{100\ \mu L\ seed}$, (C) $GNR_{200\ \mu L\ seed}$, and (D) $GNR_{400\ \mu L\ seed}$.

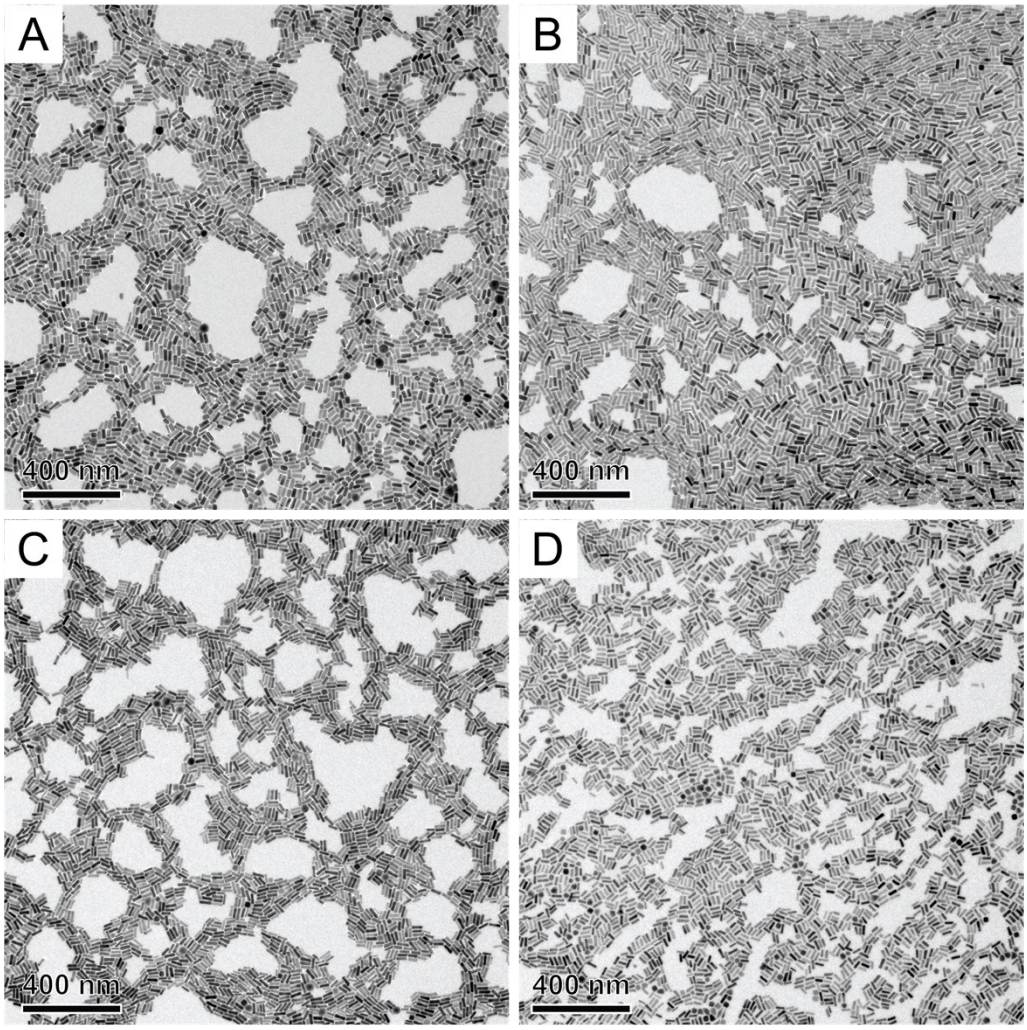

Figure S7. Low magnification TEM images of GNRs synthesized with various amounts of Ag ions. (A) $GNR_{50\ \mu L\ Ag^+}$, (B) $GNR_{100\ \mu L\ Ag^+}$, (C) $GNR_{200\ \mu L\ Ag^+}$, and (D) $GNR_{400\ \mu L\ Ag^+}$.

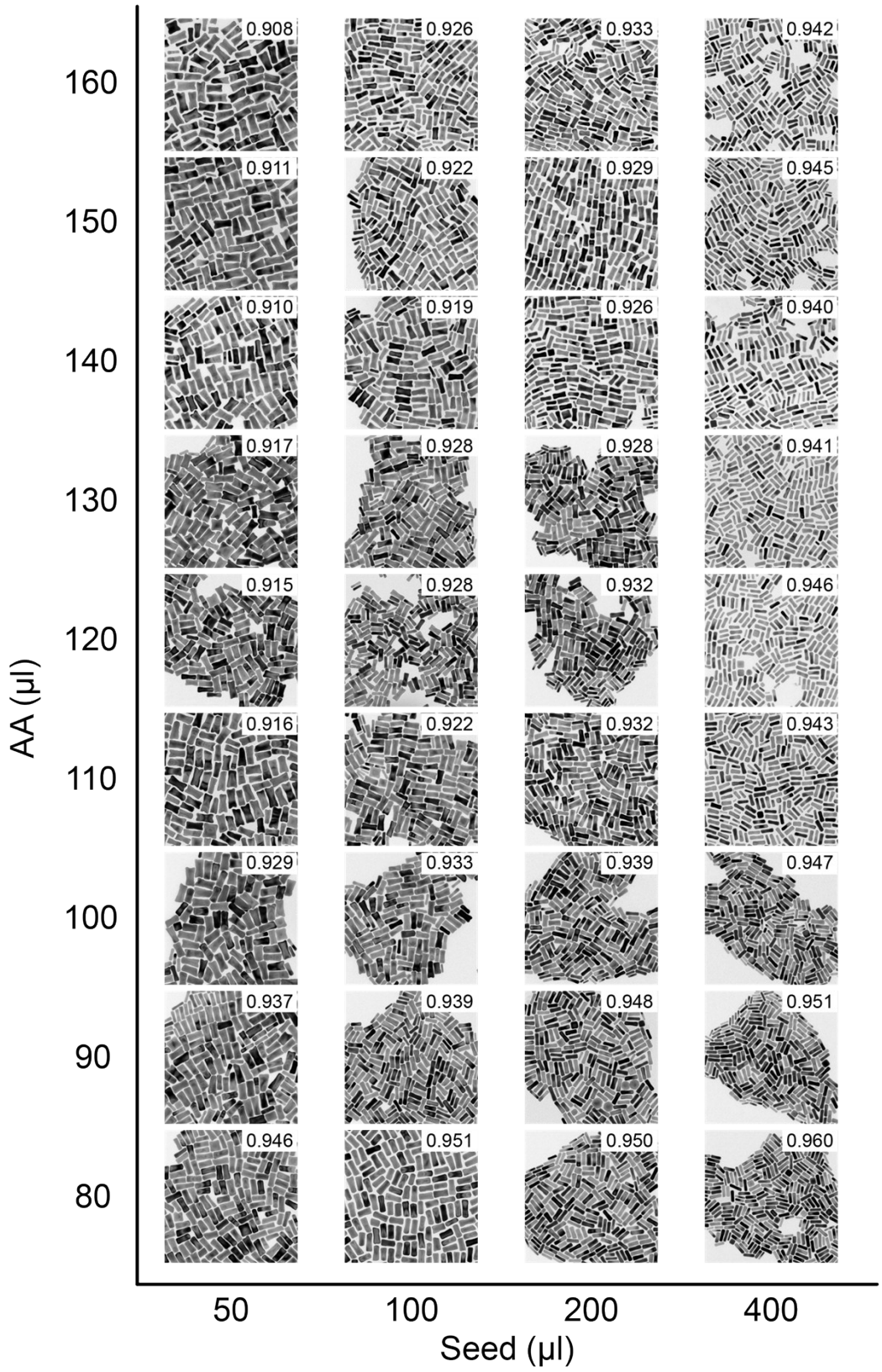

Figure S8. The change of the size and shape of GNRs synthesized with various amounts of AA and seed. Inset numbers indicate solidities of GNRs.

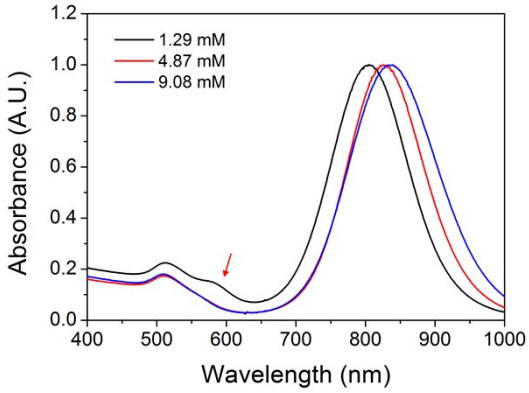

Figure S9. UV-vis spectra of GNRs synthesized with various concentrations of 2,6-dihydroxybenzoic acid. In low 2,6-dihydroxybenzoic acid condition (1.29 mM), small peak at 590 nm appears. This means that significant amount of impurities were generated during GNR synthesis.[1]

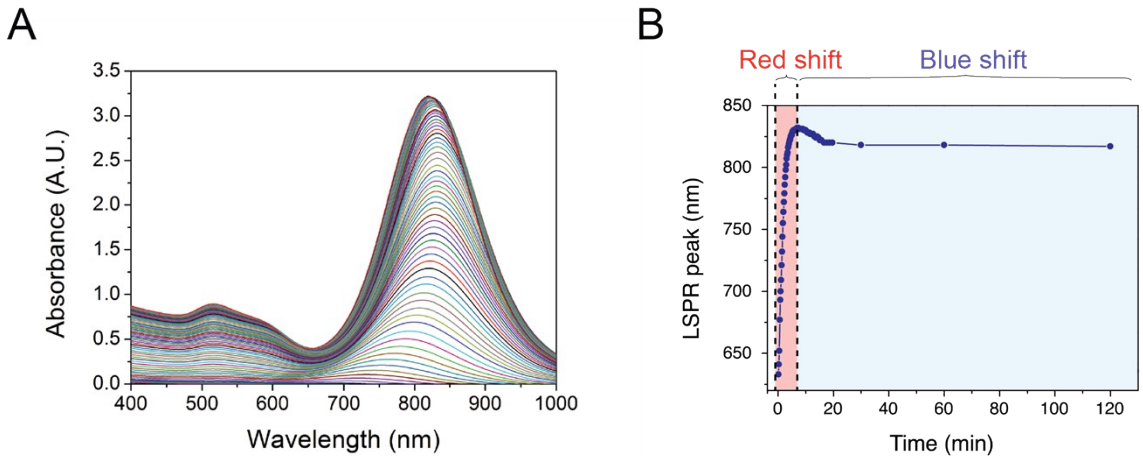

Figure 10. (A) A real time UV-vis spectroscopy characterization during early stage of GNR synthesis. (B) Localized surface plasmon resonance (LSPR) peak profile during GNR synthesis. The LSPR peak initially red-shifts but blue shifts after approximately 10 min. The LSPR peak remains stable after 2 h.

References

1 L. Scarabelli, A. Sánchez- Iglesias, J. Pérez- Juste and L. M. Liz- Marzán, *J. Phys. Chem. Lett.*, 2015, **6**, 4270–4279.